Manufacturing and Characterization of Controlled Foaming of Single Layers in Bilayer Constructs Differing in Pore Morphology

Mersa Saatchi,[1,2,3] *Marc Behl*,[1,3] *Andreas Lendlein**[1,2,3]

Summary: Bilayer porous constructs from degradable polymers are considered as scaffold materials with beneficial elastic properties for cell culture application in tissue engineering. Here, we explored whether such bilayer constructs, in which only one layer was porous while the other layer enhanced the compressive mechanical properties, could be created by specific foaming of one layer with supercritical carbon dioxide ($scCO_2$). The bilayer constructs of a poly(*L*-lactide) (PLLA) and a poly(ε-caprolactone) (PCL) layer were prepared by sequential injection molding and subsequent specific foaming with $scCO_2$. Foaming conditions of $T = 45\,^{\circ}C$ and $P = 100$ bar resulted in the formation of a porous PCL layer and a non-porous PLLA layer. When the time intervals of the foaming process were increased the pore size was increased and the shape of the pores was changed from a circular to an unidirectional lamellar shape, which reduced the compressive elastic modulus of the porous PCL layer. Furthermore, the foaming process increased the adhesion force between the PLLA and PCL layers, which was attributed to a higher degree of diffusion of molten PCL into the PLLA layer. In summary, it was demonstrated that $scCO_2$ foaming is a suitable method for the creation of layered scaffolds with only one foamed layer, in which the compressive elastic modulus and pore morphology of single porous layers can be controlled by the time interval of $scCO_2$ process.

Keywords: layered structure; poly(ε-caprolactone); poly(L-lactide); scaffold; supercritical carbon dioxide

Introduction

Poly(*L*-lactide) (PLLA) and poly(ε-caprolactone) (PCL) are biodegradable materials, which have a high application potential for polymeric scaffolds.[1–3] However, the preparation of scaffolds providing high porosity and mechanical strength compared to the surrounding tissue is still a challenge.[4,5] The compressive strength and the elastic modulus, in addition to the scaffolds stiffness could be increased by reinforcing elements, such as bioactive ceramics, fibers as well as layers to the scaffold matrix.[6,7,8,9] The incorporation of a compact PLLA layer in a PLLA scaffold, which was prepared by solid liquid phase separation and freeze-drying enhanced both compressive elastic modulus and compressive strength.[10,11]

Motivated by the potential toxicity of traces of the organic solvent, which might be left in a process employing organic solvent, we explored whether such bilayer constructs could be prepared in an organic solvent free process. $ScCO_2$ foaming is a non-toxic, low-cost process to introduce pores into solid polymers and consists of

[1] Institute of Biomaterial Science and Berlin-Brandenburg Center for Regenerative Therapies, Helmholtz-Zentrum Geesthacht, Kantstraße 55, 14513 Teltow, Germany
E-mail: andreas.lendlein@hzg.de
[2] Institute of Chemistry, University of Potsdam, 14469 Potsdam, Germany
[3] Tianjin University–Helmholtz-Zentrum Geesthacht, Joint Laboratory for Biomaterials and Regenerative Medicine

four steps: a) polymer plasticization due to $scCO_2$ diffusion into polymer matrix at high pressure, b) nucleation of bubbles and generation of pores upon depressurization, c) nucleation growth due to gas diffusion from the surrounding polymer, and d) fixation of pores as a result of increased glass transition temperature (T_g). [12–14]

In this way porous structure from semi-crystalline PCL can be prepared in a $scCO_2$ foaming process at a temperature around 40 °C.[12,14] In contrast, semi-crystalline PLLA features a low crystallization rate, which results in an amorphous, glassy state as injection molding has a rapid cooling rate. However, subsequent treatment with $scCO_2$ in the foaming process induces crystallization of lactide polymer chain segments, which hinder the diffusion of $scCO_2$ into the polymer matrix causing a non-porous structure.[15–17]

Here, it was explored whether bilayer constructs could be prepared, in which only the PCL layer is foamed by taking advantage of the different crystallization kinetics. In this way, the usage of potentially toxic organic solvents for the creation of scaffolds can be avoided. Sequential injection molding of PCL and PLLA was applied to create two layer constructs, on which the foaming by $scCO_2$ was explored. The foaming process was characterized by determining the morphology of the pores in the foamed layer and the mechanical properties of the layers. The non-porous layer was characterized by tensile tests and wide angle X-ray scattering. In addition, influence of the foaming condition was studied by determining the adhesion force between the two layers.

Experimental Part

Materials: PLLA (*meso*-lactide content 8mol%, $M_w = 116{,}000\ g \cdot mol^{-1}$, $T_g = 58\ °C$, $T_m = 160\ °C$) was purchased from NatureWorks (Ingeo™ 3052D, Nebraska, USA). PCL ($M_w = 123{,}000\ g \cdot mol^{-1}$, $T_g = -60\ °C$, $T_m = 60\ °C$) was obtained from Perstorp (CAPA® 6800, Cheshire, UK). The materials were received as pellets and were used without any further purification.

Bilayer formation: The double layer constructs composed of PLLA and PCL layers were manufactured by sequential injection molding with a HAAKE Minijet machine (Thermo Electron Corporation, Newington, NH, USA). At first, a PCL layer was injected in a mold of test specimens type DIN EN ISO 1BB (length = 20 mm, width = 2 mm, thickness = 1 mm). After cooling, the prepared PCL layer was placed in a mold of similar shape but doubled thickness (length = 20 mm, width = 2 mm, thickness = 2 mm). PLLA was injected on the top of the PCL layer yielding a bilayer construct.

Controlled foaming of PCL layer: Bilayer constructs, in which only the PCL layer was foamed, were obtained by placing the double layer constructs in a $scCO_2$ autoclave as described in reference.[18] The constructs were placed in glass vials as sample vessels in the autoclave. Two different time intervals (1 h and 4 h) were applied, whereby pressure and temperature were kept constant (100 bar, 45 °C). Figure 1 illustrates the formation process and provides process parameters.

Characterization methods: The weight average molecular weight (M_w) of PLLA and PCL were analyzed by gel permeation chromatography (GPC). Multi detector GPC measurements were performed using chloroform at 35 °C as eluent with a flow rate of $1\ mL \cdot min^{-1}$ and 0.2 wt% toluene as internal standard to monitor the flow. The GPC system consisted of a precolumn, two 300 mm x 8.0 mm linear M columns (Polymer Standards Service GmbH, Mainz, Germany, PSS), an isocratic pump 2080, and an automatic injector AS 2050 (both Jasco, Tokyo, Japan). Two detectors were used: a RI detector Shodex RI-101 (Showa Denko, Japan) and the dual detector T60A (Viscotek Corp., USA), which were combined by a split. Molecular weights were determined by universal calibration applying polystyrene standards with M_n between $580\ g \cdot mol^{-1}$ and $975\,000\ g \cdot mol^{-1}$ (PSS) using the SEC software Unity (PSS). M_w

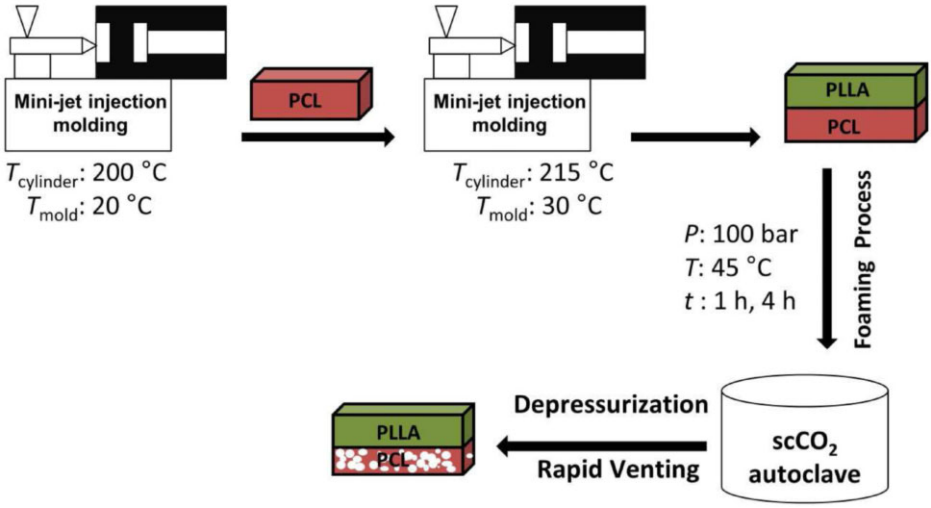

Figure 1.
Schematic presentation of the sequential injection molding for the formation of bilayer constructs and the subsequent controlled specific foaming process.

of the PLLA and the PCL layers were determined after each process step.

The thermal properties of PLLA and PCL after each process step were characterized by differential scanning calorimetry (DSC) (Netzsch DSC 204 Phoenix, Netzsch, Selb, Germany) from -10 to 200 °C with a heating rate of 10 $K \cdot min^{-1}$.

Morphological analysis of the double layer constructs were carried out by scanning electron microscopy (SEM). Cross sections of the samples were coated by a 4 nm conductive layer and images were taken at 50 - 2000X, 3 kV using Zeiss Supra 40 VP (Zeiss, Jena, Germany). The porosity and pore size were determined by X-ray computed microtomography (μ-CT, Procon X-ray GmbH, Garbsen, Germany). The single porous layer was fixed on a rotary stage and scanned inside the μ-CT apparatus using a voltage of 40 kV and a current of 0.19 mA.

Wide angle X-ray scattering (WAXS) measurements were performed at room temperature on a Bruker D8 Discover (Bruker AXS, Karlsruhe, Germany) to investigate the formation of crystalline domains in PLLA layers. The X-ray generator was operated at 40 kV and 40 mA on a copper-anode. The collimator was adjusted to 0.8 mm beam size. The two-dimensional detector (Hi-Star) was operated in 1024 × 1024 pixel mode. The distance sample-detector was 150 mm and the wavelength $\lambda = 0.15418$ nm. The detector was positioned at an angular positions $2\theta = 25°$ in order to cover an angular range from $2\theta = 7.2°$ to 43.5°. Exposure time was 300 s per scattering pattern.

Compression tests of single PCL porous layers were carried out on a Z005 Zwick (Zwick GmbH, Ulm, Germany) at room temperature. The porous structures were compressed up to 50% strain to measure the compressive elastic modulus followed by the unloading of the compressive stress to determine the elastic recovery of the pores.

Single PLLA layers were tested under tensile condition on a Z005 Zwick (Zwick GmbH, Ulm, Germany) with a strain rate of 5 $mm \cdot min^{-1}$ at room temperature.

Adhesion force between the two layers was examined with the Z005 Zwick tensile tester (Zwick GmbH, Ulm, Germany) by a T-Peel test [19] with a peeling rate of 20 $mm \cdot min^{-1}$ at room temperature.

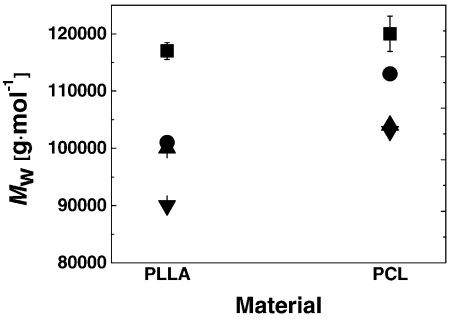

Figure 2.
Effect of different processing methods on the M_w of the polymer in each layer. M_w: ■ starting material; ● after injection molding; ▲ after foaming process for 1 h; ▼ after foaming process for 4 h.

Results and Discussion

The double layer constructs were named as BL(X), single layers of PLLA and PCL were defined as LPLA(X) and LPCL(X) and in addition, X indicated the time interval of foaming process in hours. M_w and thermal properties of PLLA and PCL layer were compared after each process step to the M_w and thermal properties of the starting material for exploring the degradation caused by heat and shear forces during the process. When the time intervals of the foaming process were increased from 1 h to 4 h the M_w of PLLA was decreased by 1000 g·mol^{-1} while the M_w of the PCL layer was not significantly influenced (Figure 2). Additionally, exposure to the $scCO_2$ autoclave did not influence the thermal properties of PLA and PCL layers (Figure 3).

Furthermore, when the time interval of the foaming process in the autoclave was extended from 1 h to 4 h, the shape of the pores determined by SEM was altered from a circular shape to an unidirectional lamellar shape (Figure 4). In addition, the average size of the pores increased from $190 \pm 90\,\mu m$ to $220 \pm 90\,\mu m$ while the porosity remained constant at $80 \pm 5\%$. The $scCO_2$ foaming process induced crystalline domains in the PLLA layer from 0% (before $scCO_2$ process) to $50 \pm 10\%$ (after 1 h) and $33 \pm 5\%$ (after 4 h), which were further explored by WAXS measurements (Figure 5a). The lateral crystal size of the induced crystalline domains was determined as 8 ± 1 nm (after 1 h) and 16 ± 1 nm (after 4 h). Injection molding of PLLA prepared with a rapid cooling rate led to the formation of an amorphous solid. The exposure to high pressure during the $scCO_2$ foaming process induced crystalline domains, which was attributed to a reduction of T_g and rearrangement of polymer chains. These effects stabilized the amorphous domains and resulted in the formation of a non-porous PLLA layer. The Young's modulus of non-porous PLLA layers decreased from 1700 ± 100 MPa (before $scCO_2$ process) to 1600 ± 100 MPa

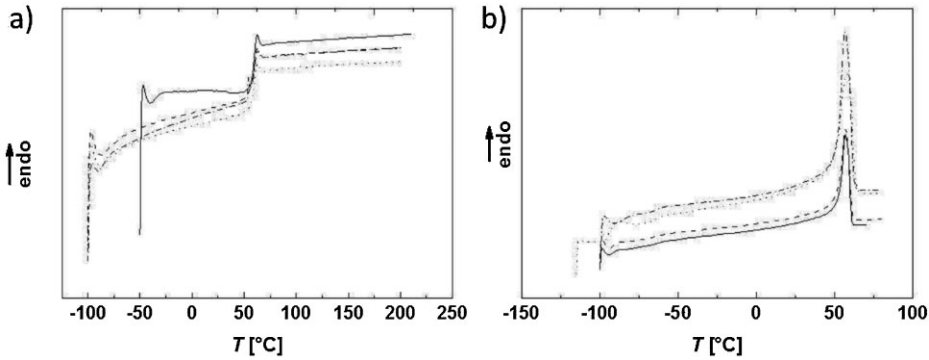

Figure 3.
Effect of the different processing methods on the thermal properties of the polymer in each layer. DSC thermograms of a) – starting material of PLA; - ·-·- PLA after injection molding; ···· LPLA(1); --- LPLA(4), b) ···· starting material of PCL;-·-·-PCL after injection molding; – LPCL(1); --- LPCL(4) on the second heating cycle.

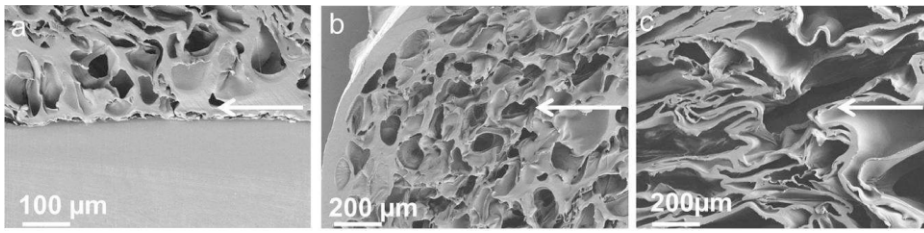

Figure 4.
SEM images of the double layer constructs. a) Double layer construct of BL(1), in which the PCL layer was foamed and the PLLA layer remained compact. b) Porous layer LPCL(1) with circular shaped pores. c) Porous layer of LPCL(4) with pores providing an unidirectional lamellar shape. Arrows indicate the direction of foaming.

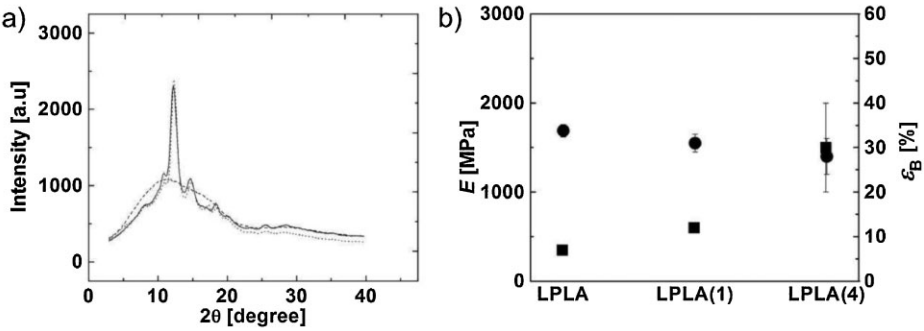

Figure 5.
a) WAXS analysis of PLLA before and after foaming process. –– LPLA; ⁻⁻⁻ LPLA(1); ···· LPLA(4). b) Tensile tests of PLLA before and after foaming process. ● E; ■ ε_B.

(after 1 h) and 1400 ± 100 MPa (after 4 h) as determined by tensile tests (Figure 5b). On the other hand, the elongation at break (ε_b) of non-porous PLLA layers increased from $7 \pm 1\%$ (before $scCO_2$ process) to $12 \pm 1\%$ (after 1 h) and $30 \pm 10\%$ (after 4 h). These results can be explained by the formation of crystalline domains and a correspondingly increased lateral size of the crystals during the foaming process (Table 1).

The mechanical properties of the PCL porous layer were analyzed by compression tests (Figure 6a). LPCL(1) exhibited a compressive elastic modulus (E_{comp}) of 2300 ± 500 kPa and an elastic recovery of $45 \pm 3\%$. However, for LPCL(4) E_{comp} and elastic recovery were reduced to 700 ± 100 kPa and $25 \pm 4\%$, respectively. When the time intervals of the foaming process was extended from 1 h to 4 h two differently shaped porous structures in the porous layers were obtained, which highly affected E_{comp} and elastic recovery. A compression up to 50% caused the bending of the circular pore walls. However, the deformation of the unidirectional lamellar pores led

Table 1.
Characterization of the PLLA layer before and after exposure in the $scCO_2$ autoclave.

Layer ID	DOC[a,b] [%]	Lateral crystal size[b] [nm]	E[c] [MPa]	ε_b[d] [%]
LPLA	0	0	1700 ± 100	7 ± 1
LPLA(1)	50 ± 10	8 ± 1	1600 ± 100	12 ± 1
LPLA(4)	33 ± 5	16 ± 1	1400 ± 100	30 ± 10

[a] Degree of crystallinity; [b] Determined by WAXS; [c] Young's modulus determined by tensile tests at room temperature; [d] Elongation at break determined by tensile tests at room temperature.

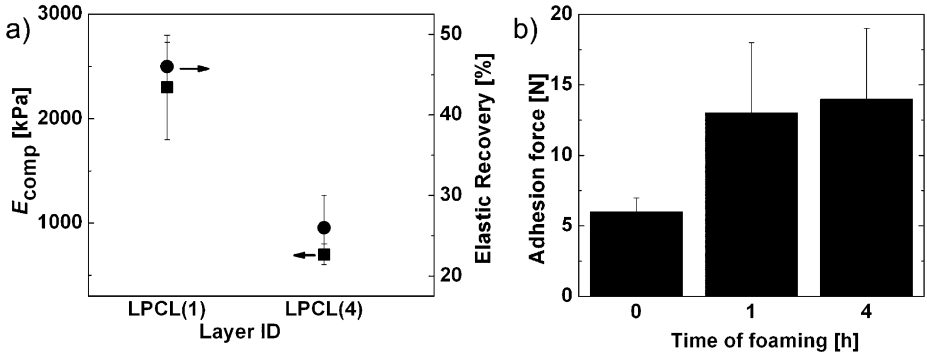

Figure 6.
a) Compression tests of the PCL porous layers ■ E_{comp}; ● Elastic recovery; b) T-Peel test of the bilayer constructs.

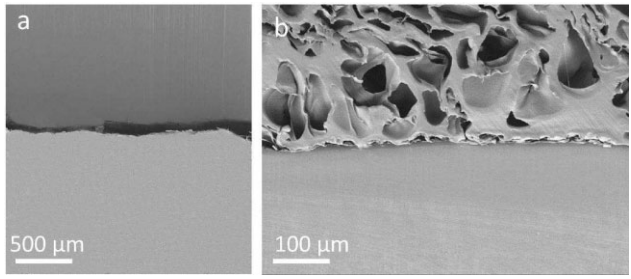

Figure 7.
SEM images of the bilayer construct interphase a) before and b) after applying $scCO_2$ conditions resulting in the foaming of the PCL layer.

to localized failure of the wall structure, which resulted in a lower E_{comp} and the elastic recovery.[20] The adhesion force between the PCL and PLLA layers was studied by T-Peel tests. Here, the adhesion force between the layers increased from 6 ± 1 N (before the foaming process) to 13 ± 4 N after the foaming process (Figure 6b). This can be attributed to a higher degree of diffusion of PCL into the interphase (on the micro level) of the bilayer constructs, which was confirmed by comparing SEM images of the bilayer constructs interphase before and after the foaming process (Figure 7).

Conclusion

Bilayer scaffolds could be obtained in a process without any organic solvent by controlled foaming of one layer of the bilayer constructs by rapid depressurization of $scCO_2$. In this way usage of potentially toxic solvents was avoided. When the time interval of the foaming process was increased the shape of the pores in the single porous layer could be tailored from circular pores to unidirectional lamellar pores, which caused the decrease of the compressive elastic modulus from 2300 ± 500 kPa to 700 ± 100 kPa. On the other hand, the $scCO_2$ process induced crystalline domains (50%) in the non-porous layer, which increased the ε_b from 7 ± 1 to 30 ± 10%. In addition, the adhesion between both layers was increased from 6 ± 1 N to 13 ± 4 N during the foaming process. In this way the controlled foaming of one layer of the bilayer constructs might enable new reinforced scaffolds in tissue engineering.

[1] W. Guobao, X. M. Peter, *Biomaterials.* **2004**, *25*, 4749.
[2] L. Xiaoming, F. Qingling, C. Fuzhai, *Mater. Sci. Eng. C.* **2006**, *26*, 716.
[3] Y. Kang, G. Yin, Q. Yuan, Y. Yao, Z. Huang, X. Liao, B. Yang, L. Liao, H. Wang, *Eur. Polym. J.* **2008**, *43*, 2029.
[4] T. Weigel, G. Schinkel, A. Lendlein, *Expert Rev. Med. Devices.* **2006**, *6*, 835.
[5] L. J. Gibson, M. F. Ashby, G. N. Karam, U. Wegst, H. R. Shercliff, *Proc. Math. Phys. Eng.* **1995**, *450*, 141.
[6] G. Georgiou, L. Mathieu, D. P. Pioletti, P. Bourban, J. E. Månson, J. C. Knowles, S. N. Nazhat, *J. Biomed. Mater. Res. Part B Appl. Biomater.* **2006**, *80*, 322.
[7] S. D. Mccullen, C. M. Haslauera, E. G. Loboa, *J. Mater. Chem.* **2010**, *20*, 877.
[8] Y. Kang, A. Scully, D. Young, S. Kim, H. Tsao, M. Sen, Y. Yang, *Europ. Polym. J.* **2011**, *47*, 1569.
[9] J.-E. Park, M. Todo, *J. Mater. Sci.* **2010**, *45*, 3966.
[10] J. E. Park, M. Todo, *Adv. Mater.* **2010**, *12*, 3303.
[11] J.-E. Park, M. Todo, *J. Mater. Sci. Mater. Med.* **2011**, *22*, 1171.
[12] A. Barry, M. Silva, V. Popov, M. Shakesheff, M. Howdle, *Phiosl. Trans. R. Soc. A.* **2006**, *364*, 249.
[13] H. Haugen, J. Will, W. Fuchs, E. Wintermantel, *J. Biomed. Mater. Res. Part B Appl. Biomater.* **2006**, *77*, 65.
[14] M. Jenkins, *Europ. Polym. J.* **2006**, *44*, 3145.
[15] T. Tabi, E. Sajo, *Express Poly. Lett.* **2010**, *4*, 659.
[16] B. Drumright, P. Gruber, D. Henton, *Adv. Mater.* **2002**, *48674*, 1841.
[17] D. Garlotta, *J. Polym. Environ.* **2002**, *9*, 63.
[18] K. Luetzow, F. Klein, T. Weigel, R. Apostel, A. Weiss, Andreas. Lendlein, *J. Biomech.* **2007**, *40*, S80.
[19] M. Mantel, F. Descaves, *J. Adhes. Sci. Technol.* **1991**, *6*, 357.
[20] M. Todo, H. Kuraoka, J. Kim, J. Taki, M. Ohshima, *J. Mater. Sci.* **2008**, *43*, 5644.

